JOURNAL OF MECHANICAL ENGINEERING AND SCIENCES (JMES)
ISSN: 2289-4659 e-ISSN: 2231-8380
VOL. 14, ISSUE 2, 6679 – 6689
DOI: https://doi.org/10.15282/jmes.14.2.2020.11.0523

ORIGINAL ARTICLE

Magnetic field enhancement technique in the fluid flow gap of a single coil twin tube Magnetorheological damper using magnetic shields

A. Ganesha, S. Patil, N. Kumar and A. Murthy

Department of Mechanical and Manufacturing Engineering, Manipal Institute of Technology, Manipal Academy of Higher Education, Manipal, India.
Phone: +917411149954

ABSTRACT – Smart dampers in the automobile suspension system bring a precise balance between the ride comfort and stability through a controllable damping coefficient. Energy absorbed by a Magnetorheological (MR) damper is a dependent function of flux density in the fluid flow gap. In this paper, magnetic field enhancement technique in the form of a single cylindrical shield and sandwich cylindrical shield is incorporated in a twin tube single coil MR damper. The field strength in different configurations of MR damper having various type of shield configuration is computationally investigated. Further, the effect of shield thickness on field strength is investigated. A significant overall improvement in the magnetic field strength is observed in the MR damper configuration having copper alloy shield.

ARTICLE HISTORY
Revised: 13th Dec 2019
Accepted: 19th Dec 2019

KEYWORDS
Magnetorheological damper;
sandwich shield;
magnetostatic analysis;
twin tube;
ride comfort.

INTRODUCTION

Magnetorheological (MR) fluid is one of the famous working fluids used in smart dampers, whose viscosity can be controlled by changing the applied magnetic field. In late 1940, MR fluid was developed by Jacob Rabinow at the US National Bureau of Standards. A typical MR fluid consists of 20-40% of magnetizable particles [1]. The damping force developed by the MR damper is a function of fluid properties, geometric properties and operating conditions. The fluid properties are controlled by selecting the appropriate volume fractions, suitable additives, and a mixture of suspended particles [2, 3]. The MR fluid properties can also be enhanced by particle coating technique [4]. The design parameters such as material properties of the piston and cylinder, geometric shape, coil variables have a significant influence on the magnetic flux density developed in the fluid flow gap. However, the geometric properties and the basic fluid properties are generally not altered once the damper is assembled. The smart dampers require the real-time control of the damping coefficient. This generally achieved by controlling the current flowing through the damper coils.

In recent years the development in the computational technique helped many researchers to investigate the characteristics of different MR dampers designs. Parlak and Engin [5], considered MR fluid as non-Newtonian fluid and calculated the damping force and plug thickness through quasi-static analysis. The fluid flow in the MR damper can be modelled as the non -Newtonian fluid between two parallel plates [6]. The damping force for complex dampers can also be calculated by using computational techniques and statistical methods, which uses the total magnetic flux density in the fluid flow gap obtained from the magnetostatic analysis [7]. The piston head material of the MR damper largely affects the damping force. Gurubasavaraju et al [8], through computational investigation suggested magnetic steel and low carbon steel are the most suitable material for the piston head. The geometric properties such as fluid flow gap, number of turns in the coil, height and width of the coil a have a significant influence on the damping force offered by the damper. Design of experiment (DOE) is one of the powerful techniques to find the main effect and interaction effect of different design variables present in the MR damper. Gurubasavaraju et al [9] investigated the dominating parameters of MR damper using DOE and observed that fluid flow gap has the highest influence on the damping force. In a single coil MR damper, the magnetic flux density is high near the upper and lower part of the piston. But a large volume of MR fluid is exposed to a shadow region where the magnetic flux density is very less [10, 11]. The flux density in the flow gap can be improved by splitting a single coil into a number of small coils [12–14]. This technique makes the piston and magnetic circuit design very complex. The flux lines in an MR damper can be altered from its actual path [15–17]. A flux deviating technique to increase the damping force by using a thin layer of copper on the outer surface of the cylinder wall was proposed by Ganesha and Amarmurthy [18].

Many researchers optimized MR damper from various geometric aspects [19]. A wide range of MR damper models are available with a large volume of fluid flow gap exposing to the shadow region. Hence there is wide scope to minimize of shadow region. In this paper, a novel technique is adopted in the form of sandwich shield to enhance the magnetic flux density in the fluid flow gap of a twin tube MR damper. Further, the influence of shield thickness on the flux density is investigated for the MR damper configuration having a single shield and sandwich shield cylinder.

*CORRESPONDING AUTHOR | N. Kumar | ✉ nitesh.naik@manipal.edu

METHODOLOGY

The direct current applied to the coil of a MR damper produces a static magnetic field in the MR damper body. The geometric configurations of different MR dampers can be compared based on the magnetic field strength in the fluid flow gap. This type of comparison uses the magnetic flux density calculated using magnetostatic analysis, which considers the MR fluid also as the static nonlinear magnetic material [7]. In this study, the magnetic field developed in the flow gap of a twin tube single coil is determined through magnetostatic analysis. Figure 1 shows the flowchart of overall methodology of the investigation for the three different MR damper models. The MR damper 1 is the base model, MR damper 2 has a copper alloy shielding of 1mm in the inner surface of the inner cylinder and MR damper 3 has a shielding of 1mm copper alloy and 1mm of steel (SA1008), copper being sandwiched between the inner surface of the inner cylinder and steel shielding. Schematic representation of MR damper models is shown in Figure 2. The 3D models of these three configurations are developed in ANSYS R19 design module. Magnetic flux density in the flow gap is evaluated for the maximum current of 1A at 9V. Also, the effect of variation of shield thickness on flux density is analyzed by using the magnetostatic module of ANSYS R19.

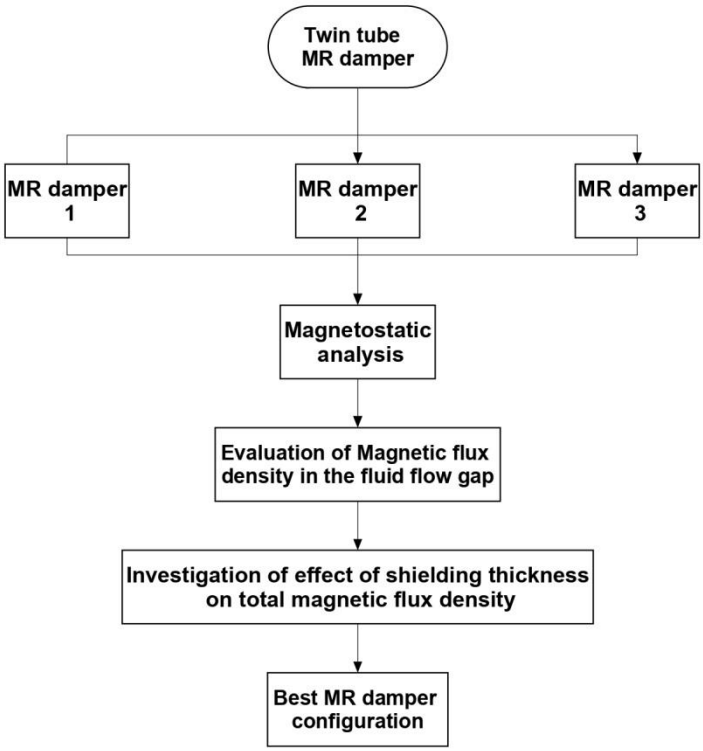

Figure 1. Methodology flowchart.

GEOMETRIC DETAILS

A twin cylinder MR damper consists of a piston having an electromagnetic coil, inner cylinder and outer cylinder. The schematic representation of MR damper 1 (base model) is shown in Figure 2 and the corresponding dimensions are shown in Table 1. The damper geometry is symmetric about two planes. Hence to reduce computational time only one quarter of the damper is considered for magnetostatic analysis.

Table 1. Parameters of MR damper [7].

Parameters of MR damper 1	Dimensions (mm)
Thickness of inner cylinder (T_1)	5
Thickness of outer cylinder (T_2)	9
Distance between poles (L)	21
Pole length (i)	2
Radial distance from piston rod to coil width (h)	7.5
Coil width (w)	5
Fluid flow gap (T_g)	1.5
Reservoir (T_R)	4

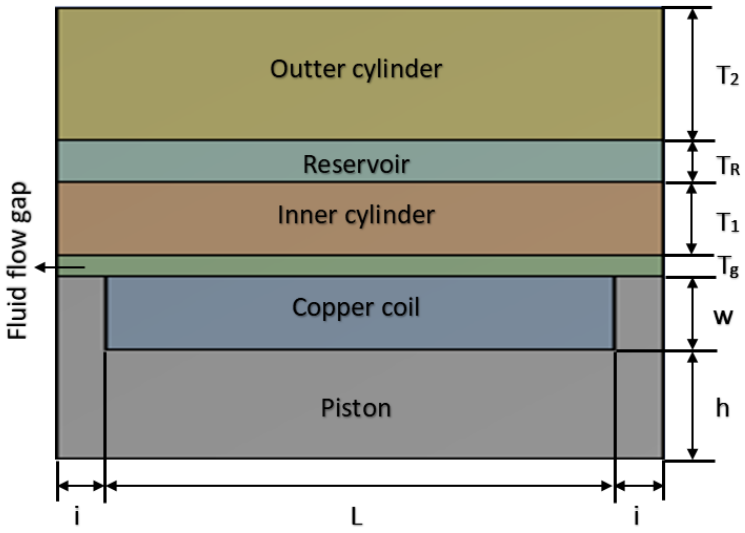

Figure 2. Schematic representation of MR damper 2D model [7].

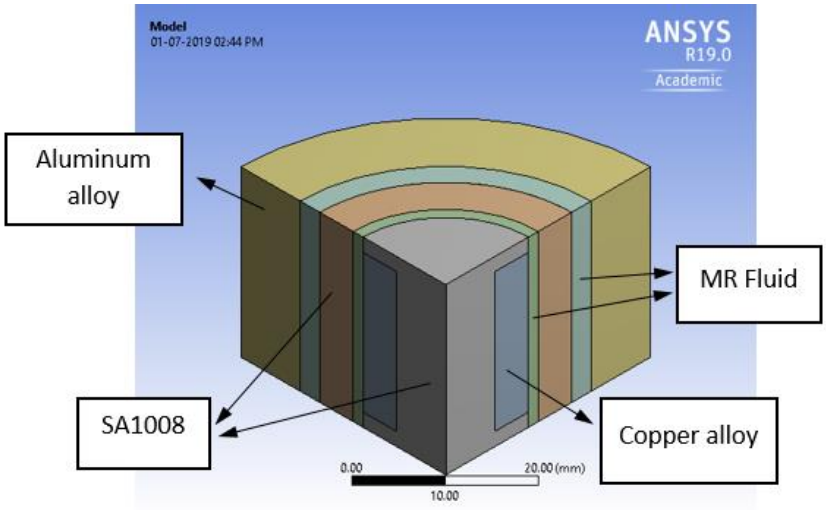

(a)

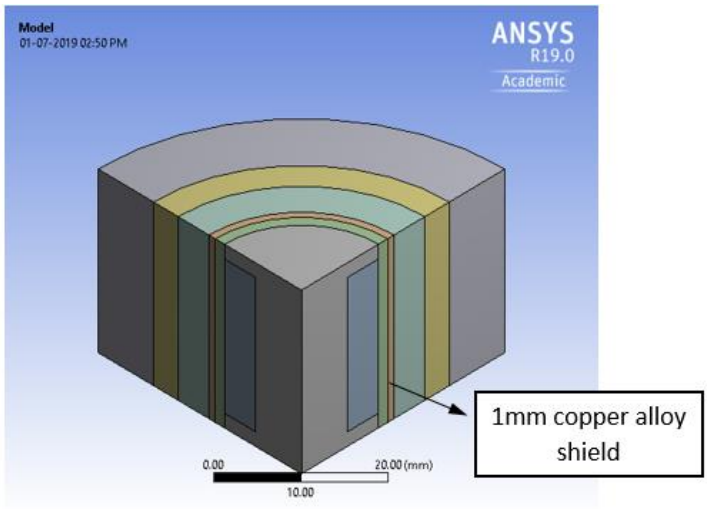

(b)

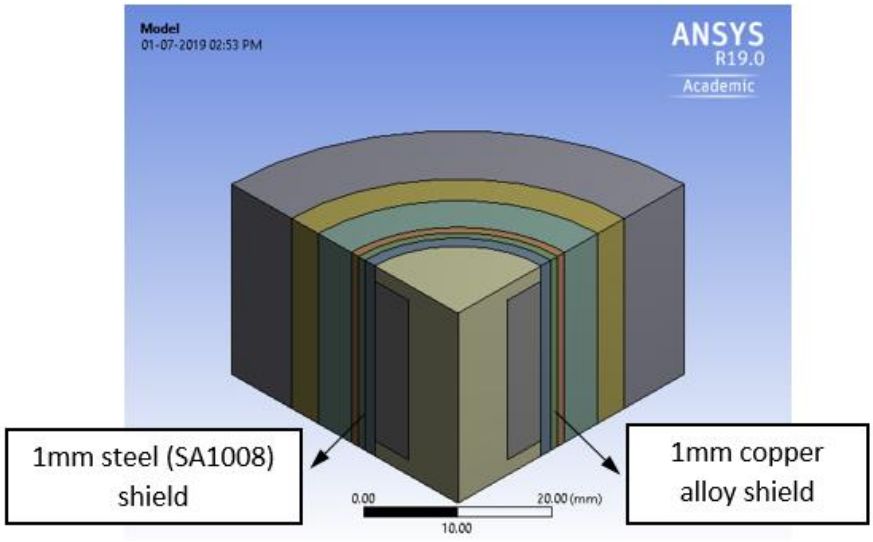

(c)

Figure 3. MR damper models: (a) MR damper 1 (Base model), (b) MR damper 2 and (c) MR damper 3.

MAGNETOSTATIC ANALYSIS

A magnetostatic analysis is generally used to solve the magnetic field resulting from a DC current. In this investigation, twin tube single coil MR damper having an electromagnetic circuit in the piston consists of 1000 number of turns and it is subjected to a maximum direct current of 1 A and 9 V electric potential. In the magnetostatic analysis, the MR damper model is enclosed inside a cubical enclosure having two plane symmetry and SOLID117 element type is used for modelling the electromagnetic computational domain. Table 2 highlights the material properties of the domains used in this analysis. The material property of the enclosure is considered as the atmospheric air. In magnetostaic analysis the electric field of the damper coil is completely decoupled from the magnetic field and the following Maxwell's equation is solved.

$$\nabla \times H = J \tag{1}$$

$$\nabla \cdot B = 0 \tag{2}$$

$$B = \mu_o \mu_r (H) \cdot H \tag{3}$$

where,

H is the magnetic field density
J is the current density
B is the magnetic flux density
μ_o is the magnetic permeability of free space ($4\pi \times 10^{-7}$ Tm/A)
μ_r is the relative permeability of the material.

Table 2. Material properties of MR damper.

Material	Relative permeability
Steel (SA1008)	B–H curve (Figure 4(a))
Copper alloy	1
MR fluid	B–H curve (Figure 4(b))
Aluminium alloy	1

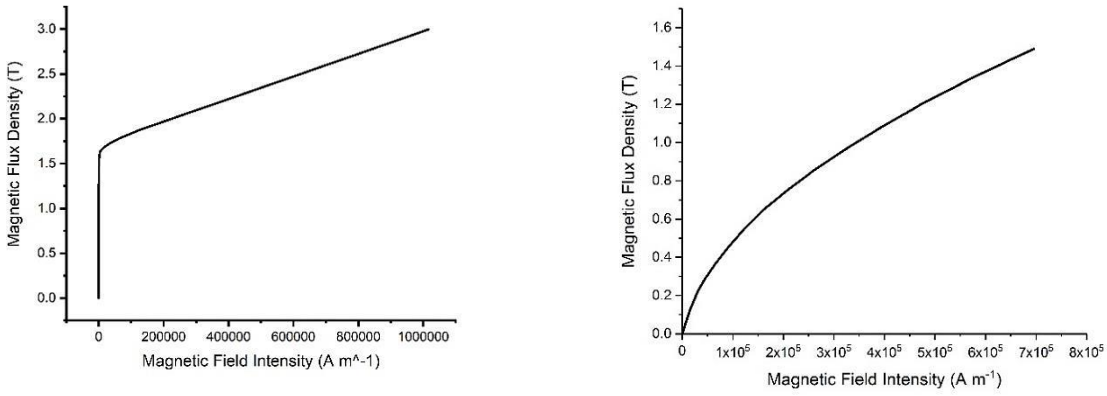

(a) (b)

Figure 4. B-H curve of: (a) SA 1008 and (b) MRF-132DG [20].

MESH DETAILS AND BOUNDARY CONDITION

A structured mesh in the fluid flow gap is obtained by sweep method and controlling the number of divisions in each edge of the geometry as shown in Figure 5. The care has been taken so that the maximum skewness is less than 0.2 in the geometry. For the interior geometry, natural boundary condition is applied, which enables a continuous H field across the boundary. The symmetric boundary condition is applied to the two symmetric planes, which will maintain the parallel flux lines and the prevents the flux line crossover. A current of 1 A at 9 V is applied to the one face of the coil as shown in Figure 6. The conductor was defined as the solid conductor having 1000 turns. The magnetic flux density in the fluid flow gap is calculated by considering different number of elements, same has been plotted in Figure 7. It has been observed that 40000 nodes in the fluid flow gap are the optimum number of nodes for computational analysis.

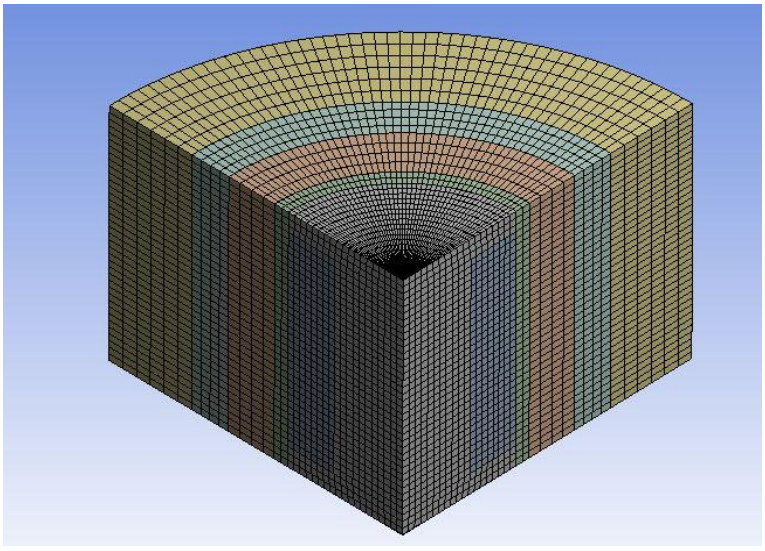

Figure 5. Meshed model of MR damper.

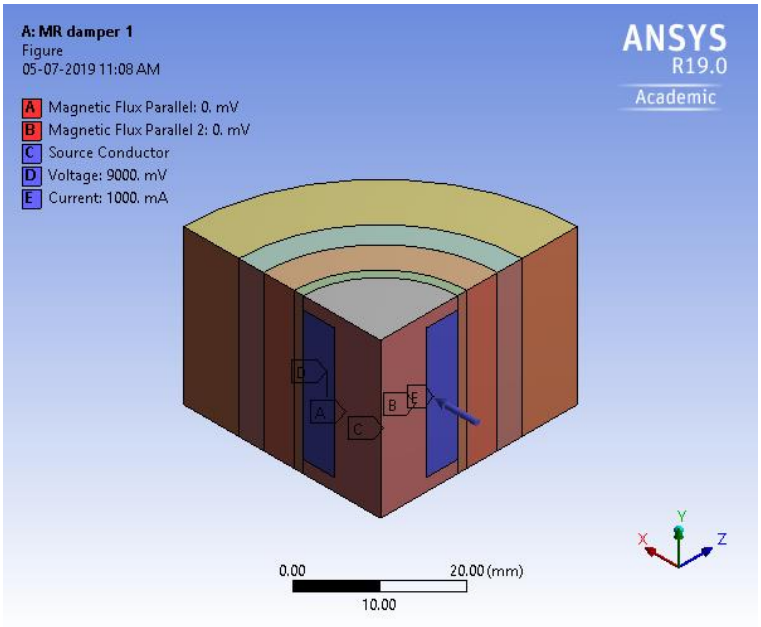

Figure 6. Boundary conditions for magnetostatic analysis.

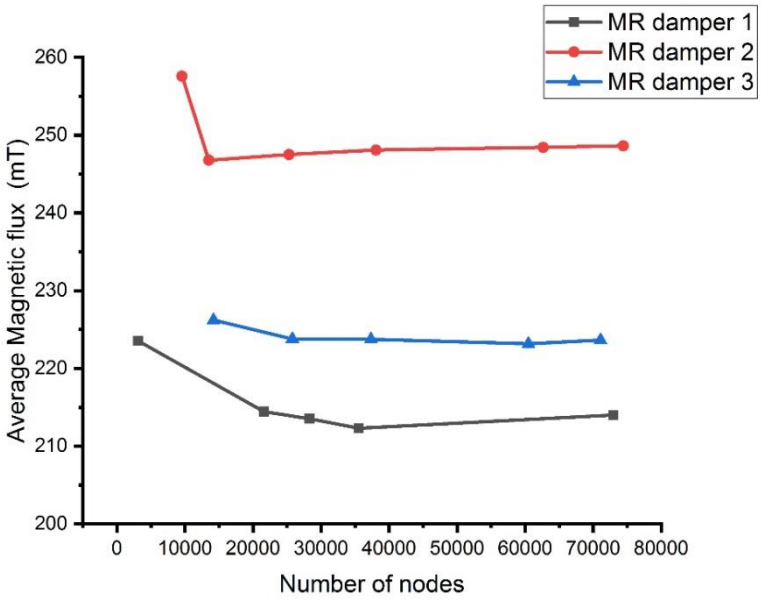

Figure 7. Grid independence test.

MODEL VALIDATION

The base model of this investigation is compared with the reference model available in the literature [7] by taking the magnetic field strength as the parameter of comparison. Three levels namely the maximum magnetic flux density, average magnetic flux density and the minimum magnetic flux density developed in the fluid flow gap are compared as shown in Figure 8. There is a quantitative match between the field strength calculated for the base model and the reference model [7] in all three levels. Hence the base model can be used as the benchmark for the geometric modification of the MR damper.

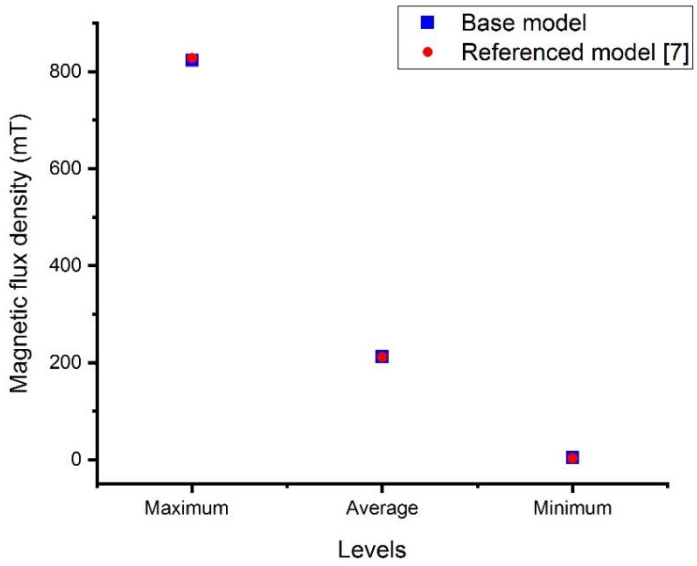

Figure 8. Model validation.

RESULTS AND DISCUSSION

The total magnetic flux density in the fluid flow gap for the three models are shown in Figure 9. Average magnetic flux density in MR damper 1 is 212.3047 mT. There is a significant improvement in MR damper 2 and MR damper 3 having average magnetic flux densities of 248.5558 mT and 223.3249 mT respectively. Even though the maximum value of the total magnetic flux of MR damper 2 is comparatively less, the minimum value of total magnetic flux has been increased drastically. In MR damper 3, the maximum value of the total magnetic flux has increased significantly with respect to MR damper 1 and MR damper 2 and minimum value of the magnetic flux density has increased compared to MR damper 1 but there is a drop in the minimum flux density value in comparison with MR damper 2.

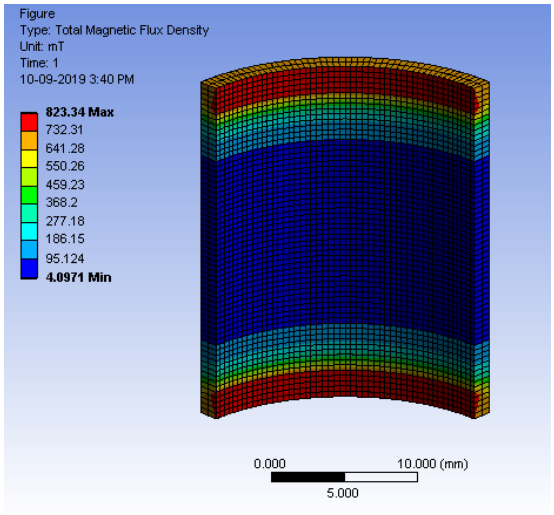

(a)

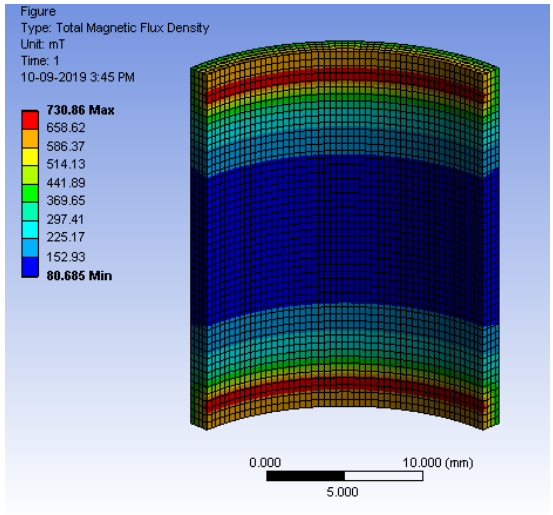

(b)

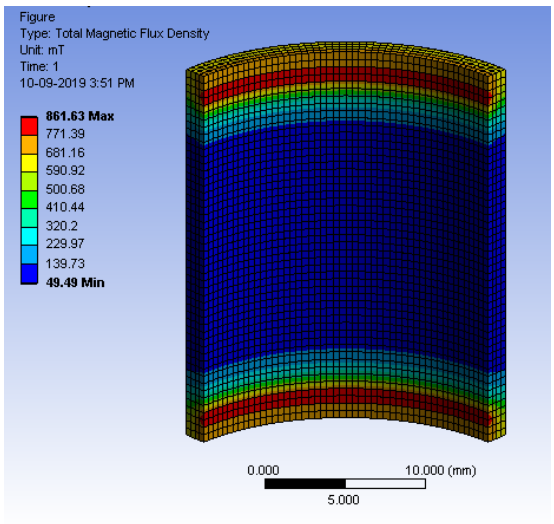

(c)

Figure 9. Flux density in the fluid flow gap: (a) MR damper 1, (b) MR damper 2 and (c) MR damper 3.

EFFECT OF SHIELD THICKNESS

Several configurations of MR damper 2 and MR damper 3 is investigated by changing the thickness of the shields. For MR damper 2, configuration modification has been done by varying the copper alloy shield thickness from 1mm to 2.5mm. The values for maximum and minimum magnetic flux density for the various models are shown in Table 3. A negative correlation has been observed between the copper shield thickness and the maximum value of magnetic flux density where as a positive correlation is observed between the minimum magnetic flux density and the copper shield thickness. Further, there is an overall improvement of 29% in the average magnetic flux density for the copper shield thickness of 2.5mm. This increase is due to the deviation of flux lines towards the fluid flow gap. The response of average magnetic flux density for different copper alloy shielding thickness is shown in Figure 10.

Table 3. Effect of thickness of the copper shield.

Model	Thickness of the copper shield (mm)	Maximum values of magnetic flux density (mT)	Minimum values of magnetic flux density (mT)	Average magnetic flux density in fluid flow gap (mT)	Percentage Improvement in comparison with base model (%)
1	1	730.86	80.685	248.5558	17.08%
2	1.5	688.24	113.73	260.8450	22.86%
3	2	655.01	139.16	260.8450	26.67%
4	2.5	628.62	158.56	273.9996	29.05%

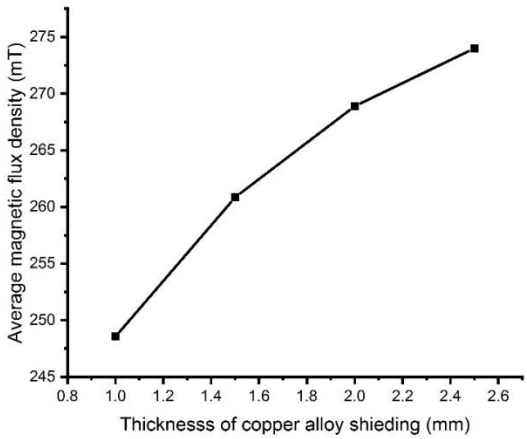

Figure 10. Effect of shield thickness on average magnetic flux density.

For MR damper 3, nine configurations are investigated by varying the shield thickness of both steel and copper alloy from 0.5 mm to 1. 5mm. The thickness of different configurations is shown in Table 4. The range of flux density value obtained in the fluid flow gap for all the configurations under investigation is shown in Figure 11.

Table 4. Configurations of MR damper model 3.

Configuration of MR damper model 3	Copper thickness (mm)	Steel thickness (mm)	Average magnetic flux density in fluid flow gap (mT)	Percentage Improvement in comparison with base model (%)
1	0.5	0.5	236.6009	11%
2	0.5	1	218.5345	2.93%
3	0.5	1.5	215.383	1.45%
4	1	0.5	248.6381	17.11%
5	1	1	223.3249	5.19%
6	1	1.5	215.5103	1.50%
7	1.5	0.5	257.738	21.40%
8	1.5	1	227.3311	7.08%
9	1.5	1.5	215.5867	1.55%

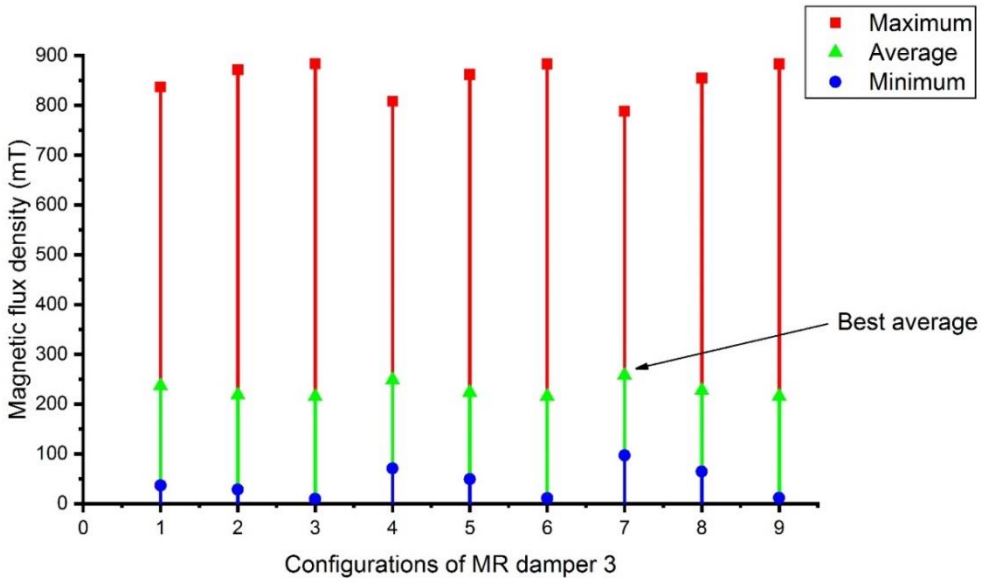

Figure 11. Magnetic flux density values for different configurations of MR damper 3.

The highest total magnetic flux density value of 883.58mT is obtained for configuration 3. A small volume of MR fluid near the upper and lower part of the piston is exposed to this value of total magnetic flux density. But a large volume of MR fluid near the coil region is exposed to the minimum total magnetic flux density of 9.3568mT. The average total magnetic flux density in the fluid flow gap is 215.383mT. On the other hand, the configuration 7 has the best average value of Total magnetic flux density of 257.738 mT. This is mainly because of the increase of minimum total magnetic flux density to 97.125mT. For a constant copper alloy shield thickness damper model, an increase in the steel shield thickness will result in the increase maximum magnetic flux density but minimum. But for the same configuration, the minimum value of magnetic flux density will decreases. The response of the average value of total magnetic flux density to the steel shield thickness variation for a constant copper alloy thickness is plotted in Figure 12. For a constant copper alloy shield, an increase in the thickness of the steel shield shows a negative correlation. At a 1.5mm thickness of steel shield, the variation in the copper alloy thickness has no significant effect on average total magnetic flux density value. But for the lower thickness steel shield between the range 0.5 to 1.5mm, the increase in the copper alloy shield appreciates the average flux density in the fluid flow gap.

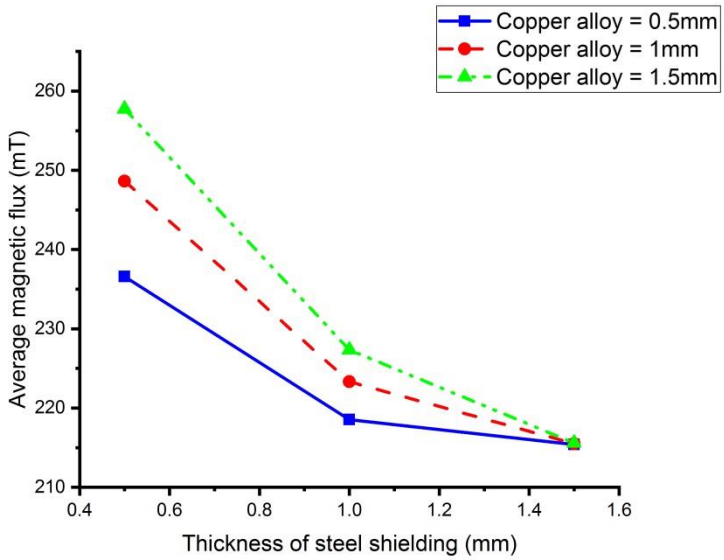

Figure 12. Response of average flux density to the shield thickness variation.

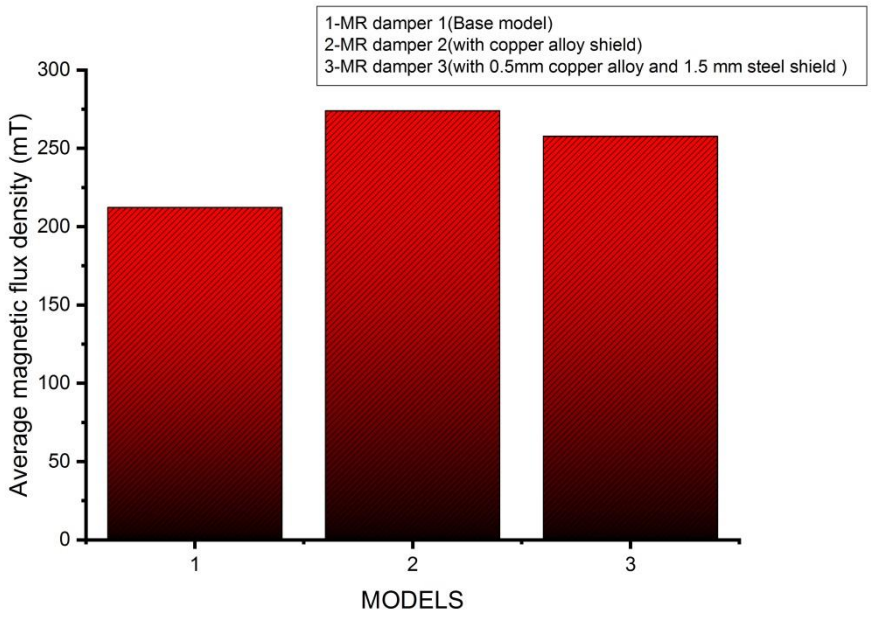

Figure 13. Average magnetic flux density comparision of best models.

A graphical comparison of best models of single shield MR damper and the sandwich MR damper with the base model taking average magnetic flux density developed in the fluid flow gap as the parameter of comparison is shown in Figure 13. Both the models result in better average magnetic flux density than the base model. Further, the MR damper with a single copper alloy shield of 0.5 mm thickness shows better performance than the sandwich model having the copper alloy shield thickness of 0.5 mm and the steel shield thickness of 1.5 mm

CONCLUSION

In this work, the effect of shield and sandwich shield on the total magnetic flux density in the fluid flow gap of a twin tube single coil MR damper is investigated through magnetostatic analysis. A positive impact of the shield on average magnetic flux density is observed due to the deviation of flux lines from the actual path. Even though the highest value of magnetic flux density was observed in MR damper model 3 having 0.5mm copper alloy shield and 1.5 mm steel shield, the best average magnetic flux density was observed in MR damper model 2 with 2.5 mm thickness copper alloy shield.

The increase in the copper alloy thickness has a positive impact on the total magnetic flux density but the magnetic saturation level of the shielding material limits the copper alloy shielding thickness at 2.5mm.

REFERENCES

[1] S. E. Premalatha, R. Chokkalingam, and M. Mahendran, "Magneto mechanical properties of iron based MR fluids," *Am. J. Polym. Sci*, vol. 2, no. 4, pp. 50–55, 2012.

[2] T. M. Gurubasavaraju, H. Kumar, and M. Arun, "Evaluation of optimal parameters of MR fluids for damper application using particle swarm and response surface optimisation," *J. Brazilian Soc. Mech. Sci. Eng.*, vol. 39, no. 9, pp. 3683–3694, 2017.

[3] M. W. Kim, W. J. Han, Y. H. Kim, and H. J. Choi, "Effect of a hard magnetic particle additive on rheological characteristics of microspherical carbonyl iron-based magnetorheological fluid," *Colloids Surfaces A Physicochem. Eng. Asp.*, vol. 506, pp. 812–820, 2016.

[4] Y. H. Kim, B. Sim, and H. J. Choi, "Fabrication of magnetite-coated attapulgite magnetic composite nanoparticles and their magnetorheology," *Colloids Surfaces A Physicochem. Eng. Asp.*, vol. 507, pp. 103–109, 2016.

[5] Z. Parlak and T. Engin, "Time-dependent CFD and quasi-static analysis of magnetorheological fluid dampers with experimental validation," *Int. J. Mech. Sci.*, vol. 64, no. 1, pp. 22–31, 2012.

[6] E. Gedik, H. Kurt, Z. Recebli, and C. Balan, "Two-dimensional CFD simulation of magnetorheological fluid between two fixed parallel plates applied external magnetic field," *Comput. Fluids*, vol. 63, pp. 128–134, 2012.

[7] K. Hemanth, H. Kumar, and K. V Gangadharan, "Vertical dynamic analysis of a quarter car suspension system with MR damper," *J. Brazilian Soc. Mech. Sci. Eng.*, vol. 39, no. 1, pp. 41–51, 2017.

[8] T. M. Gurubasavaraju, K. Hemantha, and M. Arun, "A study of influence of material properties on magnetic flux density induced in magneto rheological damper through finite element analysis," in *MATEC Web of Conferences*, 2018, vol. 144, p. 2004.

[9] T. M. Gurubasavaraju, H. Kumar, and M. Arun, "Optimisation of monotube magnetorheological damper under shear mode," *J. Brazilian Soc. Mech. Sci. Eng.*, vol. 39, no. 6, pp. 2225–2240, 2017.

[10] Z. Parlak, T. Engin, and \.Ismail Çall\i, "Optimal design of MR damper via finite element analyses of fluid dynamic and magnetic field," *Mechatronics*, vol. 22, no. 6, pp. 890–903, 2012.

[11] H. H. Zhang, C. R. Liao, W. M. Chen, and S. L. Huang, "A magnetic design method of MR fluid dampers and FEM analysis on magnetic saturation," *J. Intell. Mater. Syst. Struct.*, vol. 17, no. 8–9, pp. 813–818, 2006.

[12] D. Paul, A. Moinuddin, M. M. N. Islam, M. D. Paul, M. A. Moinuddin, and M. M. N. Islam, "Finite Element Analysis and Simulation of a Magneto-Rheological Damper," *Int. J. Innov. Res. Sci. Technol.*, vol. 1, pp. 12–19, 2014.

[13] A. Sternberg, R. Zemp, and J. C. De La Llera, "Multiphysics behavior of a magneto-rheological damper and experimental validation," *Eng. Struct.*, vol. 69, pp. 194–205, 2014.

[14] M. S. Rahmat, K. Hudha, Z. Abd Kadir, N. R. M. Nuri, N. H. Amer, and S. Abdullah, "Modelling and control of a Magneto-Rheological elastomer for impact reduction," *J. Mech. Eng. Sci.*, vol. 13, no. 3, pp. 5259–5277, 2019.

[15] M. I. M. Ahmad, A. Arifin, and S. Abdullah, "Evaluating effect of magnetic flux leakage signals on fatigue crack growth of mild steel," *J. Mech. Eng. Sci.*, vol. 10, no. 1, pp. 1827–1834, 2016.

[16] M. Tran, Z. Memon, A. Saieed, W. Pao, and F. Hashim, "Numerical simulation of two-phase separation in T-junction with experimental validation," *J. Mech. Eng. Sci.*, vol. 12, no. 4 SE-Article, Dec. 2018, doi: 10.15282/jmes.12.4.2018.17.0363.

[17] H. Yaguchi, T. Mishina, and K. Ishikawa, "A new type of magnetic pump with coupled mechanical vibration and electromagnetic force," *J. Mech. Eng. Sci.*, vol. 13, no. 3 SE-Article, Sep. 2019, doi: 10.15282/jmes.13.3.2019.01.0427.

[18] A. A. M. Ganesha. A, "Flux deviating technique to enhance the total magnetic flux density in the fluid flow gap of a monotube single coil mr damper," *Int. J. Mech. Prod. Eng. Res. Dev.*, vol. 9, no. 3, pp. 745–752, 2019.

[19] H. Krishna, H. Kumar, and K. Gangadharan, "Optimization of Magneto-Rheological Damper for Maximizing Magnetic Flux Density in the Fluid Flow Gap Through FEA and GA Approaches," *J. Inst. Eng. Ser. C*, vol. 98, no. 4, pp. 533–539, 2017, doi: 10.1007/s40032-016-0251-z.

[20] F. Imaduddin, S. Amri Mazlan, M. Azizi Abdul Rahman, H. Zamzuri, Ubaidillah, and B. Ichwan, "A high performance magnetorheological valve with a meandering flow path," *Smart Mater. Struct.*, vol. 23, no. 6, p. 65017, 2014, doi: 10.1088/0964-1726/23/6/065017.